Computer simulation of vapor-liquid equilibria of linear dipolar fluids: Departures from the principle of corresponding states

Benito Garzón, Santiago Lago,[a] and Carlos Vega
Departamento de Química Física, Facultad de Ciencias Químicas, Universidad Complutense de Madrid. 28040 Madrid, Spain

Luis F. Rull
Departamento de Física Atómica Molecular y Nuclear, Universidad de Sevilla, Aptdo 1065, Sevilla 41080, Spain

Liquid-vapor equilibrium of linear dipolar fluids has been determined by using the Gibbs ensemble simulation technique. Several elongations and values of the dipole moment were considered. Dipole moment increases the critical temperature and affects slightly the critical density and pressure. Compressibility factor at the critical point decreases as the dipole moment of the molecule increases. Dipole moment provokes deviations from the principle of corresponding states. It is shown that the temperature-density coexistence curve is broadened and that the slope of the vapor pressure curve increases with increasing dipole moment. We propose a new way of reducing the dipole moment so that the increase of the critical temperature becomes almost independent on the molecular elongation. We have also obtained the vapor-liquid equilibrium of models having both a dipole and a quadrupole moment. The obtained data were used to describe the behavior of some relatively complex fluids, namely, 1,1,1-trifluoroethane and 2,2,2-trifluoroethanol. Good agreement for coexistence densities and pressures was obtained. The results presented in this work for linear dipolar fluids along with previous work on linear quadrupolar fluids provide a very comprehensive view of the effect of polar forces on the vapor-liquid equilibrium of linear fluids. © *1995 American Institute of Physics.*

I. INTRODUCTION

The principle of corresponding states is one of the most useful concepts in liquid state theory. This principle first enunciated by van der Waals in 1873 states that the equation of state (EOS) of a fluid when reduced by the critical properties is the same for all substances. This principle is quite successful for describing the behavior of spherical or quasi-spherical molecules. A molecular derivation of this principle was carried out by Pitzer[1] and Guggenheim.[2] However, it was soon clear that this principle is only approximate and does not hold for all kind of substances. Deviations from the principle of corresponding states[3] were clearly visible in substances having short-range repulsive anisotropic forces (nonspherical shape) and in fluids presenting long-range attractive forces provoked by multipole moments.

From an empirical point of view, deviations from the principle of corresponding states are usually described by the *acentric factor*, introduced by Pitzer *et al.*[4] However, it is clear that a molecular understanding of the origin of the deviations from the principle of corresponding states should be preferable.

The role of the molecular shape on vapor-liquid equilibrium (VLE) of linear and simple nonlinear fluids is now well understood. Perturbation theories of nonpolar linear systems have been developed during the last decade for the two-center Lennard-Jones model[5-7] and for the Kihara model.[8-10] These theories were able to describe the effect of molecular anisotropy on VLE. Recent Gibbs ensemble Monte Carlo

(GEMC) simulations of the VLE of Gay-Berne,[11,12] Kihara,[13] and two-center Lennard-Jones[14] fluids have completed the picture of how the molecular shape provokes departures from the principle of corresponding states.

The next step is to try to understand the role of polar forces on VLE of molecular fluids. With that purpose we have recently performed Gibbs ensemble simulations to determine the VLE of linear quadrupolar fluids.[15] From this study we learned the effect of a quadrupole moment on the VLE of a linear fluid. The next natural step is to analyze the effect of a dipole moment on the coexistence properties of a linear fluid. This is the purpose of the present work. Previous work concerning the effect of a dipole moment on VLE should be mentioned. The effect of a dipole moment on the coexistence properties of a spherical model has been studied by GEMC.[16-19] However, spherical molecules with a permanent dipole moment are not commonly found in nature. Typically, molecules having a permanent dipole moment present also a nonspherical shape. Lupkowsky and Monson have developed a perturbation theory for the two-center Lennard-Jones model with an embedded dipole moment.[20] Moreover, Dubey *et al.* have studied by computer simulation the VLE of this model and found good agreement with the theoretical predictions.[21] In this work we follow this line of work and we study the coexistence properties of a linear fluid with a permanent dipole moment. We choose the Kihara potential to describe the molecular shape and a dipole–dipole interaction term is added. The choice of the Kihara potential presents some advantages, in particular, that the VLE of both the nonpolar and quadrupolar Kihara fluids has been previously obtained from simulations.[13,15] In this way we are able to dis-

---
[a] Author to whom correspondence should be addressed.

cuss the effect of the dipole moment on the coexistence properties which is common with the work of Dubey *et al.*[21] Moreover, we can also discuss differences and similarities between the effect of a dipole moment on VLE with respect to the effect of the quadrupole moment or with respect to the role of the molecular shape.

The obtained results may be useful not only in providing an understanding of the role of polar forces on coexistence properties but describing the vapor-liquid equilibrium of real fluids as well. In an attempt to asses the ability of the dipolar Kihara model, we have applied our simulations to describe the VLE of a fluid of technical interest like the refrigerant 1,1,1-trifluoroethane.

Finally we shall consider the vapor-liquid equilibrium of linear models having both a dipole and a quadrupole moment. The behavior of these systems will be compared with that of a purely dipolar or a purely quadrupolar model. That allows to study the additivity of different multipole moments on the vapor-liquid coexistence properties of a given fluid. Simulation data of a dipolar model with quadrupole were used to describe the vapor-liquid coexistence properties of a complex fluid like 2,2,2-trifluoroethanol.

The scheme of the paper is as follows. In Sec. II the molecular model and simulation method are described. In Sec. III the results of the simulations, and the obtained results for models are described. The influence of the dipole moment upon the coexistence properties, critical parameters and departures from the principle of corresponding states is analyzed and a comparison with experimental results of 1,1,1-trifluoroethane is also given. Section IV presents the results of models having both a dipole and a quadrupole moment, and their application to the description of VLE of 2,2,2-trifluoroethanol. Conclusions to this work are presented in Sec. V.

II. SIMULATION METHOD

Let us consider a dipolar linear fluid consisting of rods of length L with an embedded point dipole μ, interacting through a potential given by

$$u(r,\omega_1,\omega_2)=u^K(r,\omega_1,\omega_2)+u^{\mu\mu}(r,\omega_1,\omega_2), \qquad (1)$$

where r is the distance between the centers of mass of the molecules and $\omega_i \equiv \{\theta_i,\phi_i\}$ stands for the polar angles of molecule i with respect to a reference frame having its polar axis aligned along the center of mass separation vector, $\mathbf{r}$. u^K is the Kihara potential,[22] given by

$$u^K(r,\omega_1,\omega_2)=4\epsilon\left[\left(\frac{\sigma}{\rho(r,\omega_1,\omega_2)}\right)^{12}-\left(\frac{\sigma}{\rho(r,\omega_1,\omega_2)}\right)^6\right] \qquad (2)$$

and $u^{\mu\mu}$ is the dipole–dipole potential,[23]

$$u^{\mu\mu}(r,\omega_1,\omega_2)=\frac{\boldsymbol{\mu}_1\cdot\boldsymbol{\mu}_2}{r^3}-\frac{3(\boldsymbol{\mu}_1\cdot\mathbf{r})(\boldsymbol{\mu}_2\cdot\mathbf{r})}{r^5}. \qquad (3)$$

In Eq. (2), $\rho(r,\omega_1,\omega_2)$ is the shortest distance between the molecular cores (see Fig. 1), ϵ is an energetic parameter and σ a size parameter. In Eq. (3), $\boldsymbol{\mu}_i$ is the dipole vector located in the center of molecule i, aligned with the molecu-
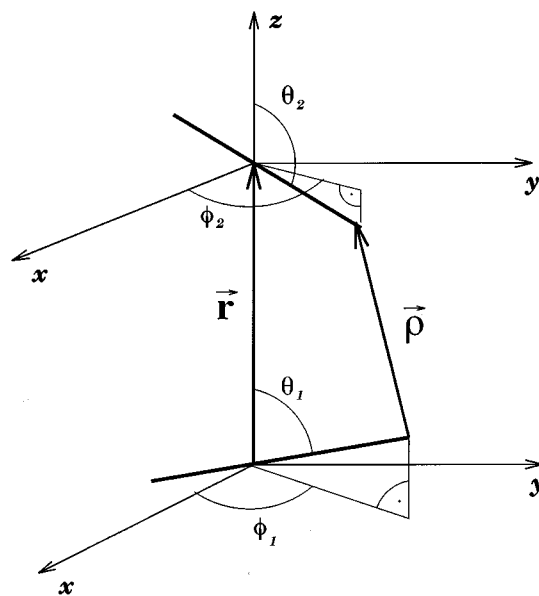

FIG. 1. Shortest distance ρ between two linear rods of length L.

lar axis. When $L=0$ and $\mu=0$, the potential function given by Eqs. (1)–(3) reduces to the well known Lennard-Jones potential. When $L=0$ and $\mu\neq0$ the fluid under consideration is the Stockmayer fluid.[23] Finally, if $L\neq0$ and $\mu=0$, we have a Kihara fluid.

The Kihara potential is a reliable model for describing thermodynamic behavior of fluids. It has been used to describe the gas,[24] liquid,[25–28] and solid phases[29] of real substances. However, we should recognize at this point that the Kihara dipolar model is somewhat artificial in one respect. Linear dipolar fluids are usually made up by heteronuclear diatomic molecules (for instance, HCl). The use of the Kihara potential given by Eq. (1) implies a spherocylinder-like core that is adequate only when the two atoms or groups forming the molecule have similar sizes. However, the use of this model presents an important advantage. Since the molecular core used is the same as in previous work on nonpolar[13] and quadrupolar[15] models any difference in the behavior of the dipolar model will be exclusively attributed to the dipole moment.

Evaluation of the Kihara potential requires the calculation of the shortest distance between two linear rods. This seems a very time consuming task, but very efficient algorithms for its determination are available,[28,30–32] so that the computer time expended in the evaluation of the Kihara potential between two linear rods is similar to the time required to evaluate the two-center Lennard-Jones interaction between two molecules.

To simulate a dipolar fluid, one has to deal with the long-range dipolar interactions. Two methods have been designed to deal with long-range effects into simulations of polar fluids: the Ewald summations (EW) method[33] and the reaction field (RF) approach.[34] In the EW method, the central simulation box is surrounded by an infinite number of replicas. To consider the long-range dipolar interactions, lattice vector sums are taken over spherical shells of an infinite spherical lattice surrounded by a continuum. The RF ap-

proach replaces particles beyond a cutoff distance by a dielectric continuum. The effect of this continuum is taken into account by including a new term into the dipolar pair potential. In previous work the VLE of dipolar fluids has been determined with the GEMC technique in combination with the EW method. However, the RF technique can be implemented in GEMC simulations yielding compatible results. We have recently performed[19] GEMC of the Stockmayer[23] model (Lennard-Jones+dipole) by using the RF technique. For this potential model GEMC simulations using the EW method are also available.[16–18] Coexistence densities and pressures and critical magnitudes obtained from both methods were undistinguishable.[19] That proves that both RF and EW can be implemented in GEMC simulations yielding identical results. In this work we shall use the RF technique to account for long-range forces since it is simpler and less computationally demanding than the EW technique. This is an important factor since the simulations even in the absence of dipolar forces are already quite demanding from a computational point of view.

Within the RF geometry, the dipolar pair interaction potential is[35]

$$u_{RF}^{\mu\mu}(r,\omega_1,\omega_2) = \begin{cases} \dfrac{\boldsymbol{\mu}_1\cdot\boldsymbol{\mu}_2}{r^3} - \dfrac{3(\boldsymbol{\mu}_1\cdot\mathbf{r})(\boldsymbol{\mu}_2\cdot\mathbf{r})}{r^5} - \dfrac{2(\epsilon_{RF}-1)}{2\epsilon_{RF}+1} \\ \qquad\times\dfrac{\boldsymbol{\mu}_1\cdot\boldsymbol{\mu}_2}{r_c^3}, \quad r<r_c \\ 0, \quad r\geq r_c \end{cases}$$
(4)

where r_c is the cutoff distance and ϵ_{RF} the dielectric constant of the continuum.

To determine the VLE of dipolar linear Kihara molecules we use the Gibbs ensemble Monte Carlo simulation technique. This method, developed by Panagiotopoulos,[36] allows the direct determination of the coexistence curve, simulating simultaneously both phases. A more detailed description of this method can be found in the original papers.[36,37]

We have obtained VLE of linear dipolar Kihara fluids of reduced length $L^*=L/\sigma=0.3$, 0.6 and 0.8 using the Gibbs ensemble technique. From a previous work,[13] we know the coexistence curve of these systems for $\mu=0$. GEMC simulations of 512 molecules were performed. At temperatures close to the critical point, the initial configuration was taken from an α-N$_2$ lattice, with 256 molecules in each box. At lower temperatures, final configurations from previous runs were used. The Kihara interaction was truncated at $\rho=3\sigma$ and long-range corrections were applied by that the fluid was uniform beyond the cutoff.[38] The long-range dipolar interaction was considered within the RF geometry by including a RF term into the pair potential [see Eq. (4)], plus the addition of a RF self-term as long-tail correction.[39] The dipolar interaction was truncated at $r_c=3\sigma+L$, and the RF dielectric constant was set equal in both phases: $\epsilon_{RF}(\text{liquid})=\epsilon_{RF}(\text{vapor})=\infty$. It has been proved that this approach does not affect to the coexistence properties.[19] To obtain a point of the coexistence curve, we performed 3000–6000 steps for equilibration plus 4000–8000 steps for averages. A step consists of one attempt of moving each particle

in both phases, followed by one attempt of changing the volume and N_{ex} attempts of exchanging particles between the simulation boxes. Acceptance ratios of particle moves and volume exchanging were kept in the range 30–60 % and N_{ex} was chosen to get an exchange ratio of 1–3 %. We obtained VLE for $T\gtrsim0.75T_c$. To obtain a point of the coexistence curve, we need about 6 h of CPU time on a DEC 3000/600 workstation.

The critical temperature, T_c^*, density, n_c^*, and pressure, P_c^* were estimated by fitting the simulation data to the expressions

$$\frac{n_1^*+n_g^*}{2}=a+bT^*,$$
(5)

$$n_1^*-n_g^*=c\left(1-\frac{T^*}{T_c^*}\right)^\beta,$$
(6)

$$\ln P^*=d+\frac{e}{T^*},$$
(7)

where n_1^* and n_g^* are the liquid and vapor reduced densities ($n^*=n\sigma^3$, with n being the number density), $T^*=kT/\epsilon$ is the reduced temperature, and $P^*=P\sigma^3/\epsilon$ is the reduced vapor pressure. Equation (5) is the rectilinear diameters law.[2] In Eq. (6), we assumed a critical exponent $\beta=1/3$, close to the universal value given by the renormalization group theory.[40] Equation (7) is the Clausius–Clapeyron equation for the vapor pressure.[41] We have also estimated the acentric factor, first defined by Pitzer *et al.*,[4]

$$\omega=-\log\left(\frac{P}{P_c}\right)_{T=0.7T_c}-1$$
(8)

which is a measure widely used in Chemical Engineering of the departures from the principle of corresponding states.

III. RESULTS AND DISCUSSION

We have obtained the coexistence curve of linear Kihara fluids for the mentioned elongations and for two different values of the reduced dipole for each elongation. The reduced dipole, μ^{*2}, is defined as

$$\mu^{*2}=\frac{\mu^2}{\epsilon\sigma^3}.$$
(9)

We have studied the following systems: $L^*=0.3$ and $\mu^{*2}=1.5$, 3; $L^*=0.6$ and $\mu^{*2}=2$, 4; and $L^*=0.8$ and $\mu^{*2}=2.3$, 4.6.

The results of simulations are presented in Tables I–III, including vapor and liquid densities and pressures on the coexistence curve for different temperatures. The estimated errors were obtained from the standard deviations over blocks of 100 steps. For some temperatures, several additional runs were also performed.

In Figs. 2, 3, and 4 we compare the results of this work for $L^*=0.3$, 0.6, and 0.8, respectively, with the previous data obtained for the nonpolar Kihara model.[13] Table IV shows the critical properties (temperature, density, pressure, packing fraction, and compressibility factor) as estimated from the simulation results making use of Eqs. (5)–(7), and an

TABLE I. Results for phase coexistence properties of linear dipolar Kihara fluids of $L^*=L/\sigma=0.3$ and $\mu^{*2}=\mu^2/(\epsilon\sigma^3)=1.5$ and 3. All thermodynamic properties are given in reduced units. The numbers in parentheses indicate the uncertainty in units of the last decimal digit i.e., 0.474(11) means 0.474 ±0.011.

T^*	n_g^*	P_g^*	n_l^*	P_l^*
		$\mu^{*2}=1.5$		
1.18	0.1102(76)	0.0657(35)	0.351(23)	0.067(29)
1.16	0.0903(41)	0.0571(25)	0.362(19)	0.048(19)
1.14	0.0674(54)	0.0490(27)	0.352(23)	0.041(20)
1.10	0.0627(32)	0.0427(14)	0.4096(92)	0.046(21)
1.075	0.0548(37)	0.0384(18)	0.425(12)	0.034(17)
1.05	0.0434(32)	0.0315(18)	0.4333(89)	0.016(20)
1.025	0.0359(13)	0.026 98(86)	0.4535(85)	0.020(22)
1	0.0333(16)	0.024 35(56)	0.4690(95)	0.016(21)
0.975	0.0273(17)	0.0203(12)	0.474(11)	0.013(30)
0.95	0.021 51(96)	0.016 31(61)	0.4891(83)	0.007(20)
0.925	0.015 83(71)	0.012 56(53)	0.4978(59)	0.004(18)
0.9	0.012 67(74)	0.010 30(63)	0.5084(66)	−0.008(27)
		$\mu^{*2}=3$		
1.28	0.0653(15)	0.0475(14)	0.377(22)	0.043(42)
1.26	0.0533(25)	0.0410(16)	0.386(19)	0.021(35)
1.25	0.0447(12)	0.036 64(98)	0.373(30)	0.005(50)
1.225	0.0425(20)	0.0337(12)	0.412(19)	0.024(46)
1.2	0.0358(14)	0.029 79(82)	0.419(19)	−0.001(46)
1.175	0.0315(13)	0.0261(11)	0.444(11)	0.016(29)
1.175	0.0327(16)	0.026 70(93)	0.4358(85)	0.003(33)
1.15	0.0288(17)	0.0235(13)	0.4485(76)	−0.022(41)
1.125	0.022 57(94)	0.019 11(79)	0.4681(61)	−0.002(34)
1.1	0.018 82(87)	0.016 18(83)	0.4767(80)	−0.008(29)
1.04	0.011 57(50)	0.010 87(54)	0.4940(62)	−0.034(48)
0.975	0.008 65(61)	0.007 24(87)	0.5255(47)	−0.029(34)
0.95	0.006 05(22)	0.005 47(31)	0.5326(52)	−0.051(33)
0.925	0.004 62(15)	0.004 56(36)	0.5409(59)	−0.011(61)

TABLE II. Results for phase coexistence properties of linear dipolar Kihara fluids of $L^*=L/\sigma=0.6$ and $\mu^{*2}=\mu^2/(\epsilon\sigma^3)=2$ and 4.

T^*	n_g^*	P_g^*	n_l^*	P_l^*
		$\mu^{*2}=2$		
1.035	0.0630(24)	0.0356(19)	0.286(17)	0.035(24)
1.025	0.0588(23)	0.0343(10)	0.299(13)	0.041(29)
1.015	0.0531(19)	0.0324(14)	0.298(12)	0.031(19)
1	0.0517(28)	0.0306(14)	0.311(14)	0.032(30)
0.975	0.0383(22)	0.0249(12)	0.3209(87)	0.024(22)
0.95	0.0281(17)	0.019 33(82)	0.332(10)	0.012(23)
0.925	0.022 73(41)	0.015 84(41)	0.3476(64)	0.012(23)
0.9	0.016 62(58)	0.012 28(36)	0.350(12)	−0.015(47)
0.875	0.016 33(80)	0.011 41(37)	0.3671(64)	0.006(20)
0.825	0.009 57(30)	0.007 10(34)	0.3853(38)	−0.009(15)
0.8	0.007 03(15)	0.005 80(30)	0.3958(66)	−0.011(26)
		$\mu^{*2}=4$		
1.21	0.0978(72)	0.0446(41)	0.240(22)	0.041(15)
1.2	0.0904(71)	0.0421(40)	0.246(37)	0.035(25)
1.175	0.0602(83)	0.0356(35)	0.2705(96)	0.024(10)
1.15	0.0466(35)	0.300(11)	0.292(15)	0.025(21)
1.125	0.0382(12)	0.025 89(86)	0.3120(95)	0.014(26)
1.1	0.0337(15)	0.2297(71)	0.3242(98)	0.008(20)
1.075	0.023 11(91)	0.017 21(53)	0.3297(99)	−0.001(25)
1.05	0.020 3(11)	0.015 16(69)	0.3404(70)	−0.010(23)
1.025	0.018 6(10)	0.013 58(60)	0.3562(53)	−0.014(18)
1	0.014 61(55)	0.010 94(38)	0.3640(53)	−0.011(23)
0.975	0.010 31(48)	0.008 09(31)	0.3675(55)	−0.022(22)
0.95	0.009 25(61)	0.007 21(43)	0.3835(49)	−0.016(24)

TABLE III. Results for phase coexistence properties of linear dipolar Kihara fluids of $L^*=L/\sigma=0.8$ and $\mu^{*2}=\mu^2/(\epsilon\sigma^3)=2.3$ and 4.6.

T^*	n_g^*	P_g^*	n_l^*	P_l^*
		$\mu^{*2}=2.3$		
1	0.0575(18)	0.0314(11)	0.214(28)	0.022(20)
0.99	0.0495(42)	0.0289(14)	0.210(30)	0.028(15)
0.985	0.0489(38)	0.0279(14)	0.222(23)	0.024(17)
0.975	0.0436(32)	0.02608(93)	0.244(11)	0.027(16)
0.95	0.0422(22)	0.02396(84)	0.2706(72)	0.026(20)
0.925	0.0308(25)	0.0193(11)	0.2825(75)	0.021(18)
0.9	0.0221(18)	0.01461(96)	0.2909(92)	0.015(23)
0.875	0.0180(11)	0.012 04(67)	0.3035(59)	0.016(17)
0.85	0.016 43(66)	0.010 87(47)	0.3145(47)	0.009(14)
0.825	0.011 36(48)	0.007 89(28)	0.3227(52)	0.002(16)
0.8	0.008 91(89)	0.006 27(48)	0.3295(35)	0.002(15)
0.775	0.007 15(22)	0.005 10(19)	0.3376(43)	−0.002(22)
		$\mu^{*2}=4.6$		
1.145	0.0545(25)	0.0321(22)	0.221(13)	0.034(24)
1.135	0.0484(26)	0.0298(13)	0.233(15)	0.042(30)
1.125	0.0548(30)	0.0304(19)	0.234(14)	0.033(18)
1.1	0.0446(22)	0.0259(13)	0.256(17)	0.035(29)
1.075	0.0325(20)	0.020 78(84)	0.264(11)	0.018(12)
1.05	0.300(37)	0.0192(19)	0.2828(63)	0.010(13)
1.025	0.208(24)	0.0145(14)	0.2872(64)	0.008(16)
1	0.0158(11)	0.011 38(64)	0.2961(59)	−0.004(15)
0.95	0.011 57(41)	0.008 59(41)	0.3192(55)	0.002(19)
0.925	0.009 10(98)	0.007 05(60)	0.3243(51)	−0.006(18)
0.9	0.007 24(58)	0.006 09(39)	0.3315(63)	−0.008(20)

estimate of acentric factors. Results for the Lennard-Jones critical properties from Ref. 42 are also shown.

These results show that the critical temperature increases significantly as the reduced dipole μ^{*2} increases. Therefore, the boiling temperature of a fluid increases with the dipole moment, a fact widely quoted in general chemistry text books.[43,44] Dipole moment does not affect strongly the critical density. For moderate dipole moments the critical density is almost identical with the corresponding nonpolar model of the same elongation. For large dipole moments there is a slight decrease of the critical density. These findings agree with predictions of a van der Waals like theory of polar fluids recently proposed.[45] Moreover, the packing fraction at the critical point η_c, defined as

$$\eta_c = n_c V_m, \tag{10}$$

remains almost constant and independent on both the dipole moment and the molecular elongation. Approximately the 16% of the available volume is occupied by molecules at the critical point. In Eq. (10), V_m is the molecular volume,

$$V_m = \frac{\pi}{6}\,\sigma^3\left(1+\tfrac{3}{2}\,L^*\right). \tag{11}$$

Quadrupole and dipole moments seem to affect critical densities in a different way. Quadrupole moment increases critical density[15] whereas the dipole moment provokes a slight decrease in the critical density. Critical pressure shows a similar behavior. For moderate dipole moments the critical pressure is almost identical with that of the nonpolar model. For large dipole moments there is a slight decrease of the critical pressure. In Table IV we present values of the com-
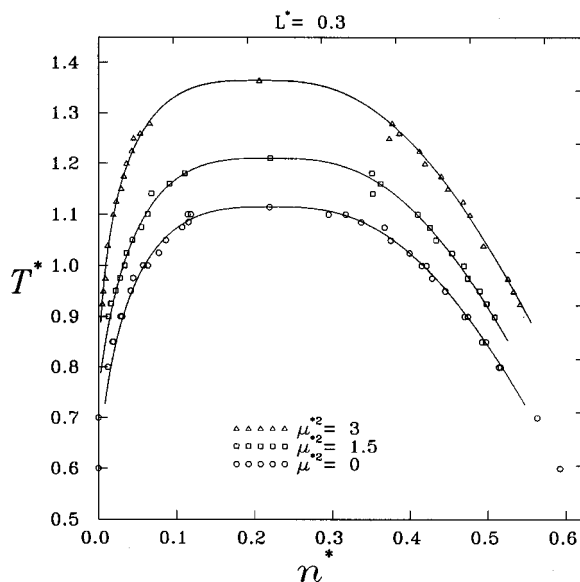
FIG. 2. Vapor-liquid coexistence densities for dipolar Kihara fluids of $L^* = L/\sigma = 0.3$. The results are given in reduced units $T^* = kT/\epsilon$ and $n^* = n\sigma^3$. Data corresponding to a reduced dipole $\mu^{*2} = \mu^2/(\epsilon\sigma^3) = 3$ are plotted with triangles. Squares correspond to $\mu^{*2} = 1.5$. Circles represent data for the nonpolar system of Ref. 13. Lines are fittings of simulation data to Eqs. (5) and (6) of main text.

pressibility factor at the critical point, Z_c. Dipole moment reduces significantly the value of Z_c. This agrees with experimental data[3] and results of Table IV provide an illustration of this fact. Dipole moment does not strongly affect either critical density or pressure. However, it provokes an important increase of the critical temperature. Therefore, the decrease of Z_c with the dipole is mostly due to the increase of the critical temperature. All the results presented here for dipolar linear fluids agree with previous findings for spherical dipolar models.[16–19]
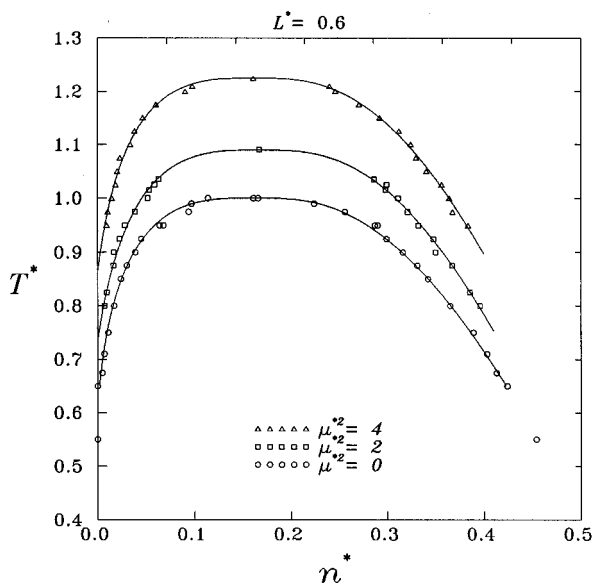
The effect of dipole moment on the vapor pressure is shown in Fig. 5 for $L^* = 0.3$. Dipole moment decreases the vapor pressure at a given temperature. The same effect is observed for the dipolar Lennard-Jones fluid.[16–19] According to the Clausius equation, which becomes accurate at low temperatures, the slope of a ln P^* vs $1/T^*$ plot is related with the vaporization enthalpy by

$$\frac{d \ln P^*}{d 1/T^*} = -\frac{\Delta H_v}{N\epsilon} = -\Delta H_v^* . \tag{12}$$

In Fig. 5 the logarithm of the reduced vapor pressure is represented vs inverse reduced temperature at different reduced dipole moments. We can conclude that since the slope of the lines is almost constant that implies, from Eq. (12), that at low temperatures ΔH_v^* is relatively constant. We see from Fig. 5 that ΔH_v^* increases as the dipole is increased. This confirms the idea (widely quoted on text books of chemistry) that vaporization enthalpy increases when molecules have a dipole moment.[43,44]

In Fig. 6(a) the relative variation of the critical temperature, $\Delta T_c/T_c^0$ for several elongations and dipole moments is shown. The magnitude ΔT_c is defined as

$$\Delta T_c = T_c(\mu^*) - T_c^0 \tag{13}$$

and T_c^0 is the critical temperature of a nonpolar model of the same elongation.

According to the results presented in Fig. 6(a) the same reduced dipole moment provokes larger changes in critical temperature as the molecule becomes more spherical. In our previous work on quadrupolar Kihara fluids,[15] we already pointed out that molecules with different elongations should be compared when they present the same *density of multipole*. In this way we were able to show that the increase of the critical temperature as a function of the density of quadrupole presents universal behavior or, in other words, is in-
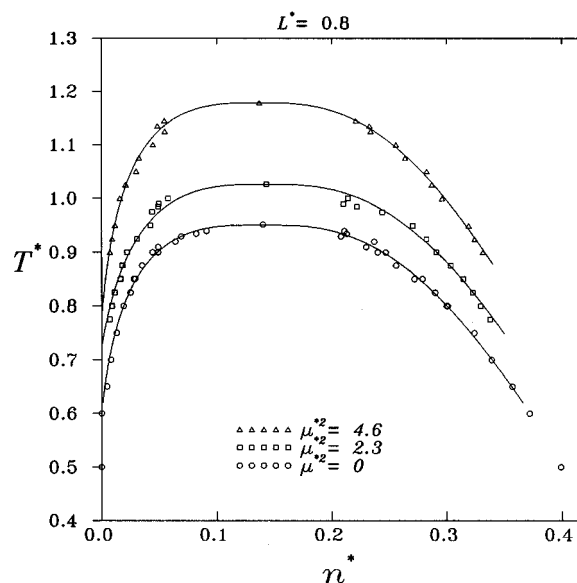

FIG. 3. Same as in Fig. 2, but for $L^* = L/\sigma = 0.6$. Data corresponding to a reduced dipole $\mu^{*2} = \mu^2/(\epsilon\sigma^3) = 4$ are plotted with triangles. Squares correspond to $\mu^{*2} = 2$. Circles represent data of nonpolar system of Ref. 13.

FIG. 4. Same as in Fig. 2, but for $L^* = L/\sigma = 0.8$. Data corresponding to a reduced dipole $\mu^{*2} = \mu^2/(\epsilon\sigma^3) = 4.6$ are plotted with triangles. Squares correspond to $\mu^{*2} = 2.3$. Circles represent data of non-polar system of Ref. 13.

TABLE IV. Critical properties of different dipolar linear fluids. η_c is the critical packing fraction, defined in Eq. (10), Z_c is the compressibility factor at the critical point and ω is the acentric factor, defined in Eq. (8).

L^*	μ^{*2}	m^2	T_c^*	n_c^*	P_c^*	η_c	Z_c	ω
0	0	0	1.310[a]	0.314[a]	0.126[a]	0.164[a]	0.306[a]	−0.03[a]
0.3	0	0	1.114(12)	0.219 (6)	0.073(10)	0.166 (5)	0.30(4)	0.00(12)
	1.5	2	1.210(40)	0.220(17)	0.075(17)	0.167(15)	0.28(9)	0.04(13)
	3	4	1.365(48)	0.206(13)	0.065(15)	0.156 (9)	0.23(5)	0.06(13)
0.6	0	0	1.000(12)	0.161 (5)	0.051(10)	0.160 (5)	0.32(6)	0.15(16)
	2	2	1.090(29)	0.167(10)	0.050(15)	0.166(10)	0.28(10)	0.15(19)
	4	4	1.225(20)	0.161(16)	0.047(13)	0.160(16)	0.24(7)	0.23(16)
0.8	0	0	0.952(11)	0.140 (3)	0.038 (8)	0.161 (4)	0.29(6)	0.11(12)
	2.3	2	1.026(24)	0.143(15)	0.037 (7)	0.165(17)	0.25(6)	0.15(11)
	4.6	4	1.179(37)	0.137(13)	0.038(13)	0.158(15)	0.24(8)	0.15(20)

[a]Results from Ref. 42.

dependent of the molecular elongation. Here we shall follow the same approach by defining the *reduced density of dipole, m*, as (see Ref. 15 for details)

$$m^2 = \frac{\mu^2}{\epsilon V_m^{3/3}}. \tag{14}$$

Figure 6(b) shows that the magnitude of $\Delta T_c/T_c^0$ follows now a universal curve as a function of m^2, regardless of the value of L^*. The universality of the curve in Fig. 6(b) supports our choice of m^2 for comparing fluids with different L^*. Consequences of the universality shown in Fig. 6(b) are quite interesting. For instance, if the critical temperature for a linear Kihara fluid with elongation L^* and $\mu^*=0$ is known (T_c^0), T_c may be predicted for any value of μ^{*2} (m^2), by reading $\Delta T_c/T_c^0$ in Fig. 6(b) and solving for T_c. The situation concerning the effect of polar forces on the critical temperature of linear fluids can be summarized as follows. For quadrupolar fluids[15] when ΔT_c (reduced by ϵ/k) is plotted as a function of the *reduced density of quadrupole* results corresponding to molecules with different elongations also fall on a single line. For dipolar fluids when $\Delta T_c/T_c^0$ is plotted as
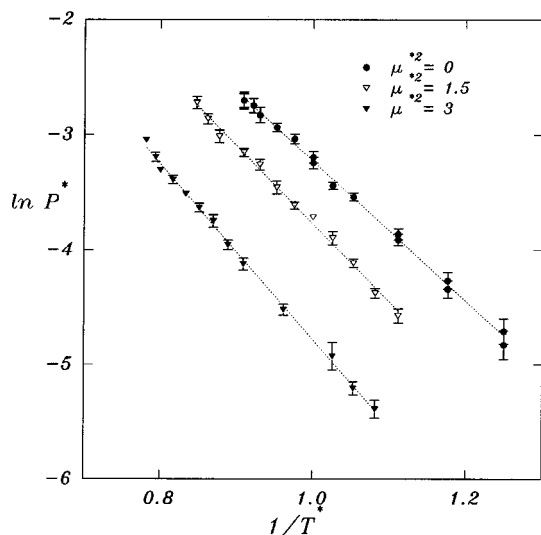

(a)

FIG. 5. Logarithm of the reduced vapor pressures, $P^* = P\sigma^3/\epsilon$ vs the inverse of reduced temperature, $1/T^* = 1/(kT/\epsilon)$, for $L^*=0.3$ and $\mu^{*2}=0$ (solid circles), $\mu^{*2}=1.5$ (open triangles), and $\mu^{*2}=3$ (solid triangles).
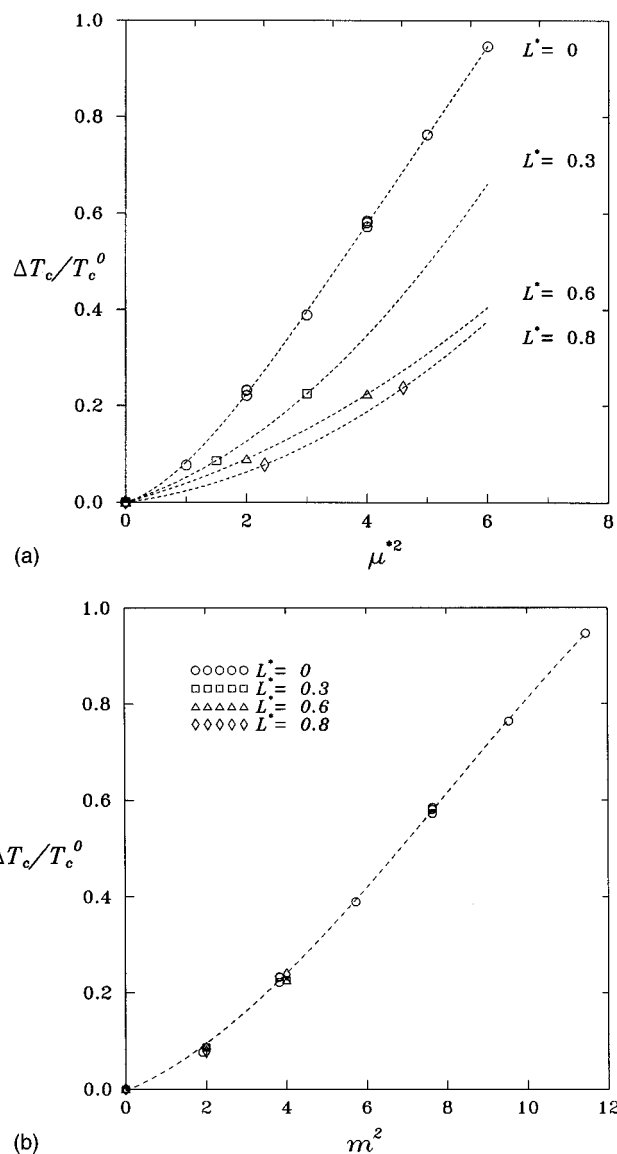

(b)

FIG. 6. (a) Relative variation of the reduced critical temperature [see Eq. (13) in the text] as a function of the reduced dipole for $L^*=0$ (circles) (results obtained from Refs. 16–19), $L^*=0.3$ (squares), $L^*=0.6$ (open triangles), and $L^*=0.8$ (open diamonds). (b) Relative variation of the reduced critical temperature as a function of the reduced density of dipole, m, defined in Eq. (14). Symbols are as in (a). Lines are plotted as a guide to the eye.
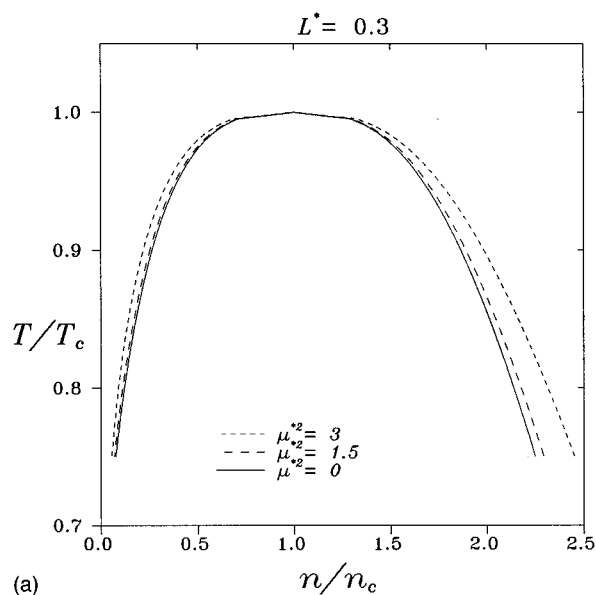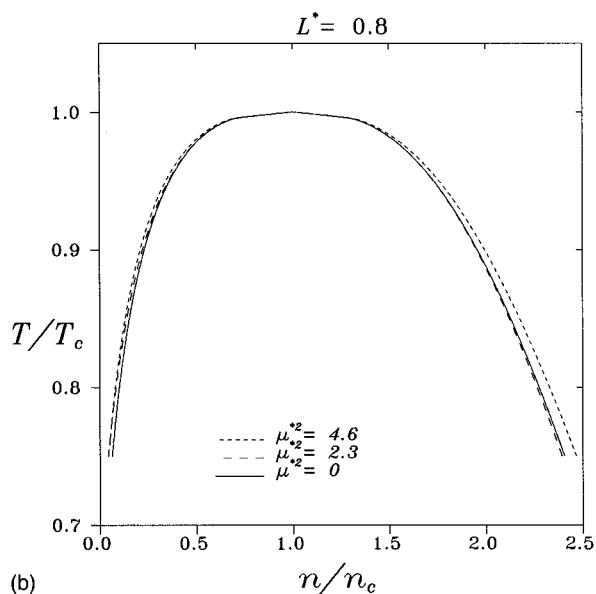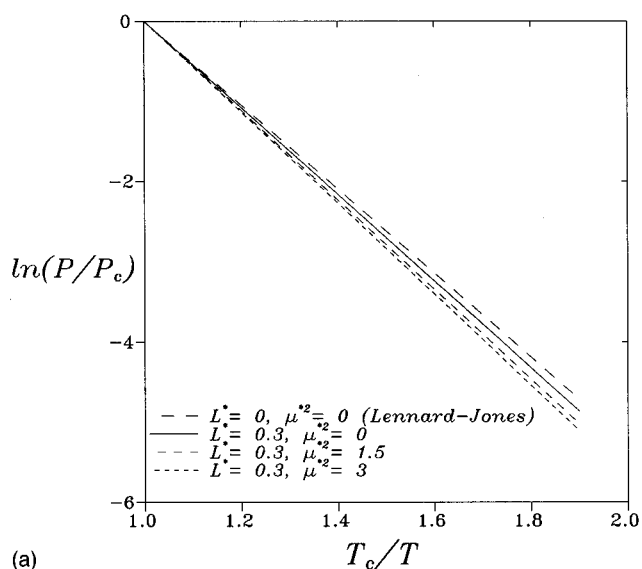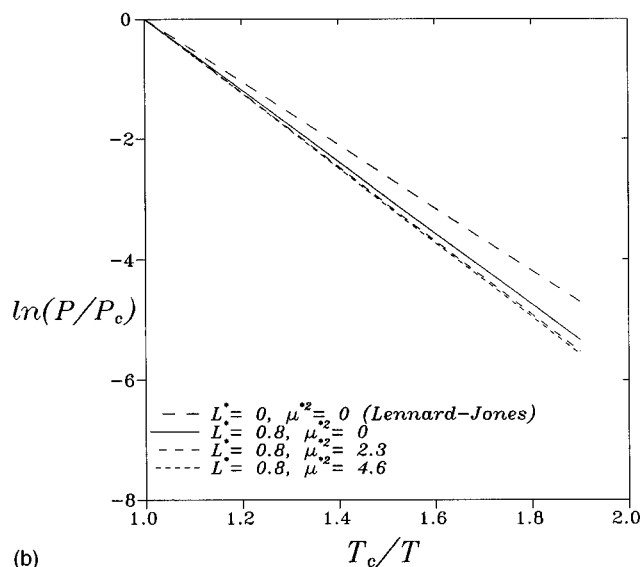
FIG. 7. Reduced coexistence densities, n/n_c, as a function of the reduced temperature, T/T_c for several dipolar systems. (a) $L^*=0.3$ and $\mu^{*2}=0$ (solid line), $\mu^{*2}=1.5$ (long-dashed line) and $\mu^{*2}=3$ (short-dashed line). (b) $L^*=0.8$ and $\mu^{*2}=0$ (solid line), $\mu^{*2}=2.3$ (long-dashed line) and $\mu^{*2}=4.6$ (short-dashed line).

FIG. 8. Reduced vapor pressures as a function of the inverse of reduced temperature for $L^*=0$, 0.3 and 0.8. (a) Results for (from top to bottom) $L^*=0$ and $\mu^{*2}=0$, and $L^*=0.3$ with $\mu^{*2}=0$, 1.5, and 3. (b) Results for (from the top to the bottom) $L^*=0$ and $\mu^{*2}=0$, and $L^*=0.8$ with $\mu^{*2}=0$, 2.3 and 4.6.

a function of the *reduced density of dipole* results corresponding to molecules with different elongations fall on a single line. The search of an explanation of these universalities should be a challenge for theories of molecular polar fluids so far presented. In fact we have recently proposed a simple theory[45] explaining some of these findings but further work is still needed.

In Fig. 7 we show the coexistence curve, when the temperature and density are reduced by their corresponding critical parameters, for two values of L^*. Although the results shown in Fig. 7 are quite sensitive to errors in the determination of critical properties, so that caution is needed, we observe that trend is a broadening of the VLE coexistence curve due to the dipole moment. Therefore, dipolar forces

provoke a broadening of the coexistence curve and this is in common with quadrupolar forces.[15]

Departures from the principle of corresponding states in the vapor pressure due to the dipole are illustrated by plots of $\ln (P/P_c)$ vs T_c/T. This is represented in Fig. 8 for $L^*=0.3$ and 0.8. We have also represented the vapor pressure of a Lennard-Jones fluid, taken from Ref. 42. Thus, it can be observed the effect that both shape and dipole exert upon deviations from corresponding states for vapor pressure. The slope (in absolute value) of the $\ln(P/P_c)$ curve increases with the molecular anisotropy (i.e., compare $L^*=0$, $\mu^{*2}=0$ with $L^*=0.3$, $\mu^{*2}=0$) also with the dipole moment (i.e., compare $L^*=0.3$, $\mu^{*2}=0$ with $L^*=0.3$, $\mu^{*2}=3$). Although these results should be taken with care due to difficulties in obtaining accurately critical magnitudes, we believe this

trend to be correct. We conclude that the effect of a dipole moment on corresponding states plots is similar to that found previously for quadrupolar models. An important property widely used in Chemical Engineering is the acentric factor ω. In the last column of Table IV computed values of ω are presented. Although a precise determination of ω from GEMC is a quite difficult task (see the large error bars of ω) some tendencies are clear. Anisotropy and dipole moment increase the magnitude of the acentric factor.

In previous work[15] we have shown that the Kihara quadrupolar model is a good effective potential for describing vapor-liquid equilibrium of real fluids. In fact the computed coexistence properties of the model were in excellent agreement with experimental results of carbon dioxide. Here we shall illustrate how this is also the case of the Kihara dipolar model. As an example we take 1,1,1-trifluoroethane (CH_3–CF_3). This choice is motivated by the fact that the size of F is similar to that of H (Ref. 46) and that makes our choice of the molecular shape (a spherocylinder) reasonable. Moreover, this molecule presents a dipole moment aligned with the C–C bond which is in common with our model. Critical temperature and density obtained from simulations for $L^*=0.6$ (a similar value of L^* was used by Fischer *et al.* to describe the thermodynamic properties of ethane[7]) and $\mu^{*2}=4$ were fitted to the experimental critical temperature and density of CH_3–CF_3. In this way we obtain the parameters $\sigma=3.73$ Å and $\epsilon/k=282.54$ K.

Experimental[47] and simulation coexistence curve and vapor pressures of the refrigerant 1,1,1-trifluoroethane are shown in Fig. 9. The dipole moment obtained with the GEMC data, $\mu_{GEMC}=2.8\times10^{-18}$ esu cm, in reasonable agreement with the experimental value,[48] $\mu=2.32\times10^{-18}$ esu cm. We have obtained an excellent description of coexistence properties of this fluid by using a simple model for its interaction energy. Therefore, we can conclude that the interaction potential of Eqs. (1)–(3) is a good effective pair potential for the thermodynamic description of a relatively complex dipolar fluid, as the refrigerant 1,1,1-trifluoroethane.

We have thus far presented results for models presenting a dipole model. In our previous work we obtained results for models presenting only a quadrupole moment. However, it is often found in nature that molecules presenting dipole moment have also a significant quadrupole moment (for instance, water).[49] In Sec. IV we present results for models having simultaneously both a dipole and a quadrupole moment.

IV. DIPOLAR MODELS WITH A QUADRUPOLE

In this section we present GEMC results for a Kihara model with $L^*=0.8$ and $\mu^{*2}=2.3$ and $Q^{*2}=1.5$. The pair potential is given by

$$u(r,\omega_1,\omega_2)=u^K(r,\omega_1,\omega_2)+u^{\mu\mu}(r,\omega_1,\omega_2)+u^{QQ}+u^{\mu Q}. \tag{15}$$

Expressions for u^K and $u^{\mu\mu}$ are given by Eqs. (1) and (2). Expression for u^{QQ} was taken from Ref. 49. The $u^{\mu Q}$ term is given by[49]
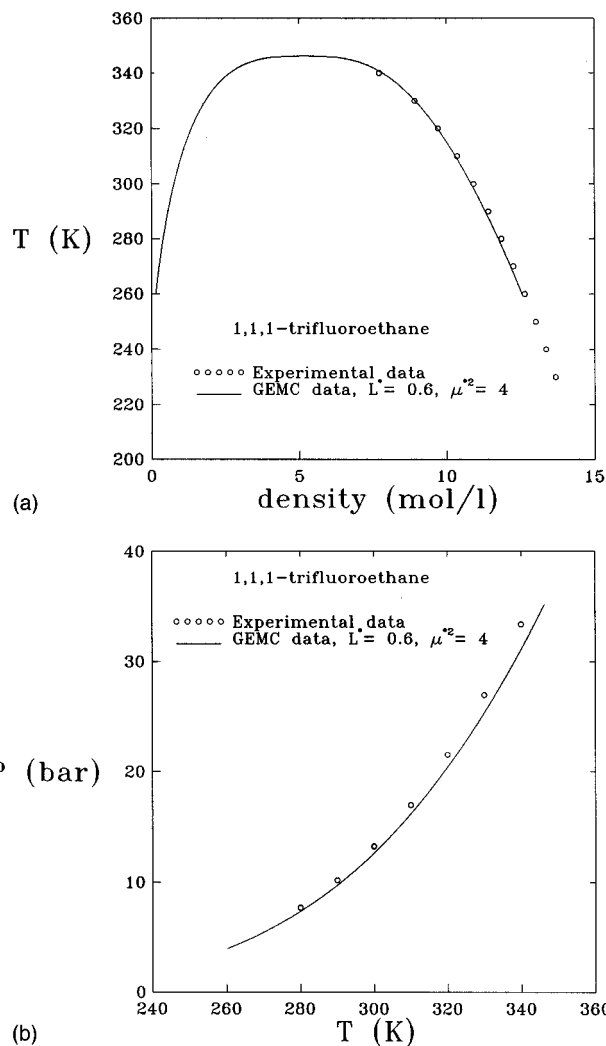

(a)

(b)

FIG. 9. Coexistence properties of 1,1,1-trifluoroethane. (a) Coexistence densities. (b) Vapor pressures. Symbols represent the experimental data (taken from Ref. 47). Lines are fittings to the GEMC data for $L^*=0.6$ and $\mu^{*2}=4$, with the parameters obtained as described in the text.

$$u^{\mu Q}=\frac{3\mu Q}{2r^4}\left[(c_1-c_2)(1+5c_1c_2-2\mathbf{e}_1\cdot\mathbf{e}_2)\right]. \tag{16}$$

In Eq. (16), $c_i=\cos\theta_i$ (see Fig. 1) and $\mathbf{e}_i$ is a unit vector in the direction of $\boldsymbol{\mu}_i$. In Table V the VLE of this model is presented. Estimated critical parameters are $T_c^*=1.153(30)$, $n_c^*=0.139(15)$, $P_c^*=0.037(8)$, and $Z_c=0.23(5)$. The acentric factor is $\omega=0.20(12)$. Results for a purely dipolar model, a purely quadrupolar and for a nonpolar model of the same elongation are also presented in Fig. 10. As expected the critical temperature of the dipole +quadrupole model is higher than that of the purely dipolar or that of the purely quadrupolar model. The value of ΔT_c^*, defined as $[T_c(\mu^*,Q^*)-T_c^0]/(\epsilon/k)$, for the dipole +quadrupole model is $\Delta T_c^*=0.201$. If the values of ΔT_c^* for the purely dipolar or the purely quadrupolar model are added then one obtains $\Delta T_c^*=0.136$. Therefore the increase of the critical temperature of the dipolar model with quadrupole is larger than the summation of the increase undergone by the purely dipolar and the purely quadrupolar

TABLE V. Coexistence properties of dipolar fluids with quadrupole. See the main text for an estimate of critical properties.

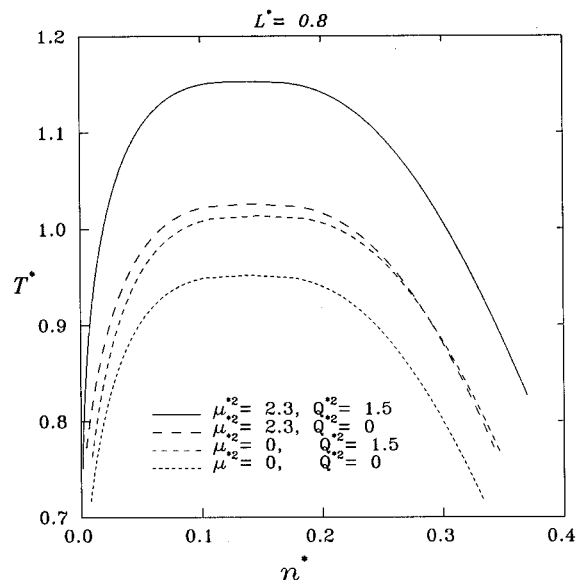| T^*	n_g^*	P_g^*	n_l^*	P_l^*
	$L^*=0.8$, $\mu^{*2}=2.3$, $Q^{*2}=1.5$			
1.1	0.0406(22)	0.0278(14)	0.234(20)	0.024(22)
1.075	0.0322(17)	0.0233(11)	0.267(13)	0.017(24)
1.05	0.0279(14)	0.0202(10)	0.2808(95)	0.017(31)
1.025	0.021 70(83)	0.016 52(70)	0.289(11)	0.009(27)
1	0.016 35(66)	0.012 68(47)	0.294(15)	0.008(54)
0.975	0.015 24(42)	0.011 45(42)	0.3173(78)	0.005(37)
0.975	0.015 63(32)	0.011 80(33)	0.3147(12)	0.000(48)
0.95	0.012 65(47)	0.009 59(40)	0.3263(93)	0.011(33)
0.925	0.010 02(54)	0.007 63(40)	0.3378(70)	−0.001(33)
0.9	0.008 36(27)	0.006 29(24)	0.3457(66)	0.001(33)
0.85	0.004 97(15)	0.003 69(12)	0.3569(59)	−0.020(36)
	$L^*=0.6$, $\mu^{*2}=1.5$, $Q^{*2}=1$			
1.07	0.0466(17)	0.0324(15)	0.296(37)	0.034(40)
1.06	0.0436(27)	0.0302(14)	0.299(25)	0.021(40)
1.05	0.0391(11)	0.0281(13)	0.312(15)	0.019(33)
1.025	0.0371(16)	0.0256(10)	0.333(12)	0.017(25)
1	0.0257(13)	0.019 27(94)	0.338(14)	0.016(31)
0.975	0.0220(10)	0.016 43(73)	0.352(13)	0.008(38)
0.95	0.0207(10)	0.015 18(61)	0.3653(79)	0.002(29)
0.95	0.0191(19)	0.0143(12)	0.3677(84)	0.006(32)
0.925	0.0157(12)	0.011 65(71)	0.3759(64)	0.002(31)
0.9	0.011 78(60)	0.008 91(41)	0.3872(74)	−0.011(34)
0.875	0.009 46(53)	0.007 13(35)	0.3946(62)	−0.006(31)
0.875	0.011 39(26)	0.008 34(22)	0.3951(65)	−0.006(36)
0.85	0.008 08(59)	0.005 95(43)	0.4060(59)	−0.003(29)
0.8	0.004 43(38)	0.003 21(27)	0.4220(50)	0.000(29)

FIG. 10. Liquid-vapor coexistence curves for polar Kihara fluids with $L^*=0.8$. Results for (from the top to the bottom) a dipolar model with quadrupole ($\mu^{*2}=2.3$, $Q^{*2}=1,5$) fluid, a pure dipolar ($\mu^{*2}=2.3$), a pure quadrupolar ($Q^{*2}=1.5$), and the nonpolar fluid. Lines are fittings to the GEMC data. Data for the pure quadrupolar fluid obtained from Ref. 15. Data for the nonpolar Kihara fluid obtained from Ref. 13.

fluid. The explanation of that is as follows. The dipolar model with quadrupole as described by Eq. (15) presents not only the u^{QQ} and $u^{\mu\mu}$ terms but also the additional contribution arising from the interaction between the dipole and the quadrupole given by the $u^{\mu Q}$ term. As a general rule terms in the Hamiltonian of a system decreasing the free energy at a given density and temperature raise the critical temperature. Conversely, terms in the Hamiltonian increasing the free energy of the system decrease the critical temperature. The terms u^{QQ}, $u^{\mu\mu}$, and $u^{\mu Q}$ decrease the free energy of the system and, therefore, all of them raise the critical temperature. The dipolar model with quadrupole is more than the summation of contributions due to the dipole and contributions due to the quadrupole and this is so because of the presence of the $u^{\mu Q}$ term. Our results agree with theoretical predictions made by Benavides *et al.*[50]

In Fig. 11 corresponding states plots of the VLE of the dipolar model with quadrupole are presented. As anticipated, the dipolar model with quadrupole presents larger deviations from the principle of corresponding states than the purely quadrupolar or the purely dipolar model. In Fig. 11(a) it can also be observed that the broadening of the coexistence curve is larger for the dipolar model with quadrupole than for the pure dipolar or quadrupolar model. Fig. 11(b) shows that the slope of the $\ln P/P_c$ vs T_c/T plot is larger for the dipolar model with quadrupole fluid.

Our conclusions are similar to the conclusions exposed by Dubey and O'Shea for Lennard-Jones dipolar plus quadrupolar fluids.[51]

As it has been already said, dipolar molecules in nature often also present a quadrupole moment.[49] To describe the liquid-vapor coexistence properties of a real dipolar fluid with quadrupole like the 2,2,2-trifluoroethanol (TFE), broadly used as solvent of proteins,[52] we have estimated the molecular parameters of a linear Kihara dipolar model with quadrupole that could give an accurate description of VLE of TFE. We have assumed the same shape for TFE than for 1,1,1-trifluoroethane, that is, $L^*=0.6$, and the same ϵ and σ Kihara parameters. Then, we have estimated the dipole and quadrupole moments of real TFE from the experimental dipole moments of 1,1,1-trifluoroethane and ethanol. By assuming a discrete charge model we have estimated that the multipole moments of real TFE are $\mu_{TFE}=1.8\times10^{-18}$ esu cm and $Q_{TFE}=5.2\times10^{-26}$ esu cm^2. The trial reduced multipole moments obtained by that way for TFE are $\mu^{*2}=\mu_{TFE}^2/(\epsilon\sigma^3)\cong1.5$ and $Q^{*2}=Q_{TFE}^2/(\epsilon\sigma^5)\cong1$. We have performed GEMC simulations of that model (see Table V). The critical parameters obtained for this model ($L^*=0.6$, $\mu^{*2}=1.5$, and $Q^{*2}=1$) are $T_c^* = 1.143(14)$, $n_c^* = 0.160(6)$ and $P_c^* = 0.050(8)$. Critical temperature and density were fitted to the experimental critical temperature and density of real TFE, obtaining the following Kihara parameters: $\epsilon/k=436.66$ K and $\sigma=3.83$ Å.

Experimental[53–56] and simulation coexistence curve and vapor pressures of TFE are shown in Fig. 12. The dipole and quadrupole moments obtained with the simulation data are $\mu_{GEMC}=2.26\times10^{-18}$ esu cm and $Q_{GEMC}=7.06\times10^{-26}$ esu cm^2, in good agreement with the estimated *experimental* multipoles. The description made by simulation of the dipolar Kihara model with quadrupole of liquid-vapor coexistence of TFE is reasonably good.

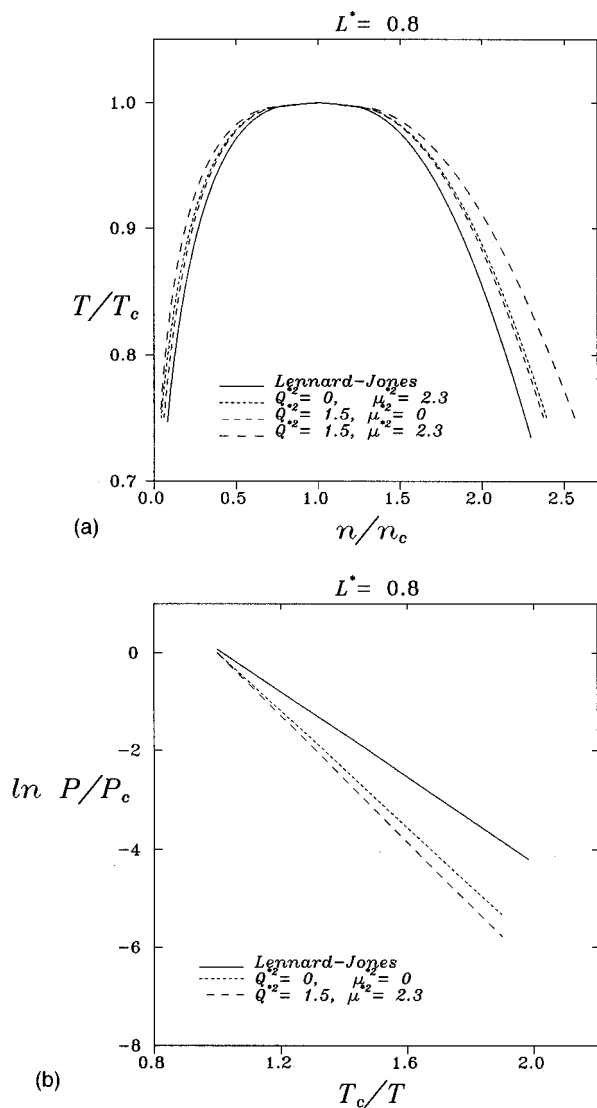A remarkable fact observed in all our simulation descrip-

(a)

(b)

FIG. 11. (a) Reduced coexistence densities, n/n_c, as a function of the reduced temperature, T/T_c for different fluids: Lennard-Jones fluid (Ref. 42) (solid line) and Kihara fluids with L^*=0.8; Quadrupolar fluid (Ref. 15) (shortest dash line), dipolar fluid (medium-dashed line) and dipolar model with quadrupole fluid (long dashed line). (b) Logarithm of the reduced vapor pressure versus inverse of reduced temperature.

The dipole moment significantly raises the critical temperature of a molecular fluid and this is in common with the effect observed in quadrupolar fluids. Critical density and pressure are not much affected by the dipole except at high dipole moments where these critical values are smaller than those found for the corresponding nonpolar model. This behavior differs significantly from that found in quadrupolar models.[15] Compressibility factor decreases with the dipole moment. This decrease is mostly due to the increase of the critical temperature since the critical density and pressure remain almost unchanged. Simulation results show that the vapor enthalpy, related with the slope of a ln P vs $1/T$ plot, is increased by the dipole moment.

We suggest a new way of reducing the dipole moment by defining the reduced density of dipole, m^2. By using the reduced density of dipole we have shown that $\Delta T_c/T_c^0$ plotted vs m^2 presents universal behavior. By universal behavior

tion of real fluids is that multipole moments obtained from simulation data overestimate systematically the multipole moments of the real fluid. The main reason of this is that experimental multipole moments are usually determined in gas phase, where polarizability effects are not present. The polarizability of molecules in the liquid phase makes a nonnegligible contribution to its properties and this contribution is present in the fitting of simulation data to the real fluid properties.

V. CONCLUSIONS

We have presented simulation results of vapor-liquid coexistence curves for dipolar linear Kihara fluids. To determine VLE, we used the Gibbs ensemble simulation technique.
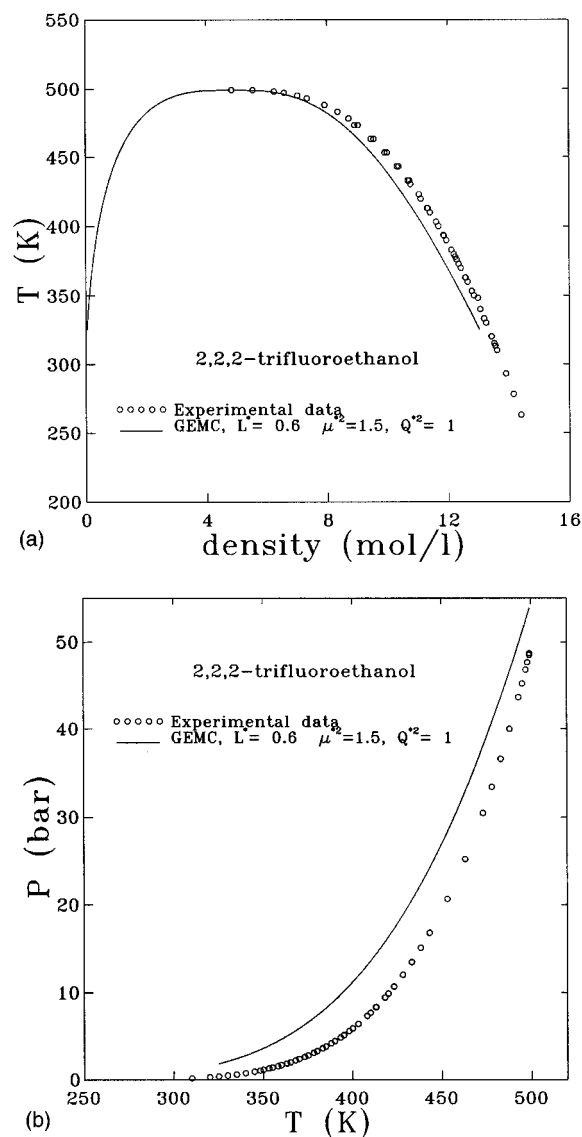

(a)

(b)

FIG. 12. Coexistence properties of 2,2,2-trifluoroethanol. (a) Coexistence densities. (b) Vapor pressures. Symbols represent the experimental data (taken from Refs. 52–55). Lines are fittings to the GEMC data for L^*=0.6 and μ^{*2}=1.5, Q^{*2}=1, with the parameters obtained as described in the text.

we mean that the results do not depend on the considered elongation. Similar universal behavior for ΔT_c^* instead of $\Delta T_c/T_c^0$ was found in quadrupolar fluids when the *reduced density of quadrupole* is used.[13] These striking findings deserve further theoretical work to understand their origin although some progress on this line has been recently done.[45,57–61]

In terms of corresponding states, we have seen that the coexistence curve is slightly broadened by the presence of the dipole. This is in common with the effect observed in quadrupolar fluids. Influence of shape and dipole upon deviations from the principle of corresponding states has also been shown by using plots of $\ln P/P_c$ vs T_c/T. The slope of this plot is related with the *acentric* factor, which has been calculated for all the simulated systems. We found that both shape and dipole increase the value of ω. This is common with the tendency reported for the quadrupolar fluid.

We have applied one coexistence curve obtained with GEMC for the dipolar Kihara model to describe the VLE of the refrigerant 1,1,1-trifluoroethane, just by fitting the potential parameters to the critical temperature and density of the refrigerant. We have obtained very good agreement between experiment and simulation data for densities and vapor pressures. This confirms the fact that the dipolar Kihara potential is a reliable effective pair potential for real fluids.

We also studied the dipolar model with an embedded quadrupole. The increase in critical temperature and deviation from the principle of corresponding states of this model are larger than those found for a purely quadrupolar or a purely dipolar model when added. The explanation of that arises from the presence of a new dipole-quadrupole interaction term. The simulation data of a dipolar Kihara model with quadrupole were used to describe the VLE of a complex fluid, the 2,2,2-trifluoroethanol, with a very good agreement between simulation and experiment.

Results of this work along with those of our previous study of quadrupolar models yield an overall picture of the effect of polar forces on the vapor-liquid equilibria of polar molecular fluids. It should be recognized, however, that a theoretical framework able to explain simultaneously all features of vapor-liquid equilibria of molecular polar fluids as described in this work is still missing and constitutes at this point a challenge.

ACKNOWLEDGMENTS

[1] K. S. Pitzer, J. Am. Chem. Soc. **77**, 3427 (1955).

[2] E. A. Guggenheim, J. Chem. Phys. **13**, 253 (1945).

[3] R. C. Reid, J. M. Prausnitz, and B. E. Poling, *The Properties of Gases and Liquids* (McGraw Hill, New York, 1986).

[4] K. S. Pitzer, D. Z. Lippmann, R. F. Curl, C. M. Huggins, and D. E. Peterson, J. Am. Chem. Soc. **77**, 3433 (1955).

[5] P. A. Monson, Mol. Phys. **53**, 1209 (1984).

[6] D. B. Mc Guigan, M. Lupkowski, D. M. Pacquet, and P. A. Monson, Mol. Phys. **67**, 33 (1989).

[7] J. Fischer, R. Lustig, M. Breitenfelder-Manske, and W. Lemming, Mol. Phys. **52**, 485 (1984).

[8] T. Boublík, J. Chem. Phys. **87**, 1751 (1987).

[9] P. Padilla, S. Lago, and C. Vega, Mol. Phys. **74**, 161 (1991).

[10] C. Vega and S. Lago, Chem. Phys. Lett. **185**, 516 (1991).

[11] E. de Miguel, L. F. Rull, M. K. Chalam, and K. E. Gubbins, Mol. Phys. **71**, 1223 (1990).

[12] E. de Miguel, L. F. Rull, and K. E. Gubbins, Physica A **177**, 174 (1991).

[13] C. Vega, S. Lago, E. de Miguel, and L. F. Rull, J. Phys. Chem. **96**, 7431 (1992).

[14] G. Galassi and D. J. Tildesley, Molec. Simul. **13**, 11 (1994).

[15] B. Garzón, S. Lago, C. Vega, E. de Miguel, and L. F. Rull, J. Chem. Phys. **101**, 4166 (1994).

[16] B. Smit, C. P. Williams, E. M. Hendriks, and S. W. de Leeuw, Mol. Phys. **68**, 765 (1989).

[17] M. E. van Leeuwen, B. Smit, and E. M. Hendriks, Mol. Phys. **78**, 271 (1993).

[18] M. E. van Leeuwen, Mol. Phys. **82**, 383 (1994).

[19] B. Garzón, S. Lago, and C. Vega, Chem. Phys. Lett. **231**, 366 (1994).

[20] M. Lupkowski and P. A. Monson, Mol. Phys. **67**, 53 (1989).

[21] G. S. Dubey, S. F. O'Shea, and P. A. Monson, Mol. Phys. **80**, 997 (1993).

[22] T. Kihara, J. Phys. Soc. Jpn. **16**, 289 (1951).

[23] W. H. Stockmayer, J. Chem. Phys. **9**, 398 (1941).

[24] T. Kihara, Chem. Phys. Lett. **92**, 175 (1982).

[25] C. Vega and S. Lago, J. Chem. Phys. **93**, 8171 (1990).

[26] P. Sevilla, S. Lago, C. Vega, and P. Padilla, Phys. Chem. Liq. **23**, 1 (1991).

[27] C. Vega, S. Lago and P. Padilla, J. Phys. Chem. **96**, 1900 (1992).

[28] C. Vega, Ph.D. thesis, Universidad Complutense de Madrid, 1991.

[29] T. Kihara and A. Koide, Adv. Chem. Phys. **33**, 51 (1975).

[30] P. Sevilla and S. Lago, Comput. Chem. **9**, 39 (1985).

[31] S. Lago and C. Vega, Comput. Chem. **12**, 343 (1988).

[32] C. Vega and S. Lago, Comput. Chem. **18**, 55 (1994).

[33] S. W. de Leeuw, J. W. Perram and E. R. Smith, Proc. R. Soc. London, Ser A **373**, 27 (1980).

[34] J. A. Barker and R. O. Watts, Mol. Phys. **26**, 789 (1973).

[35] M. Neumann, Mol. Phys. **50**, 841 (1983).

[36] A. Z. Panagiotopoulos, Mol. Phys. **61**, 813 (1987).

[37] A. Z. Panagiotopoulos, N. Quirke, M. Stapleton, and D. J. Tildesley, Mol. Phys. **63**, 527 (1988).

[38] C. Vega and D. Frenkel, Mol. Phys. **67**, 633 (1989).

[39] B. Saager, J. Fischer and M. Neumann, Mol. Simul. **6**, 27 (1991).

[40] P. Pfeuty and G. Toulose, *Introduction to the Renormalization Group and to Critical Phenomena* (Wiley, New York, 1977).

[41] I. M. Klotz and R. M. Rosenberg, *Chemical Thermodynamics* (Benjamin, Menlo Park, California, 1986).

[42] A. Lotfi, O. Vrabec and J. Fischer, Mol. Phys. **76**, 1319 (1992).

[43] L. Pauling, *General Chemistry*, 3rd. Ed. (Freeman, S. Francisco, 1970).

[44] P. W. Atkins and J. A. Beran, *General Chemistry* (Scientific America Library, New York, 1992).

[45] C. Vega, S. Lago, and B. Garzón, J. Phys. Chem. **98**, 11181 (1994).

[46] M. P. Allen and D. J. Tildesley, *Computer simulation of Liquids* (Clarendon, Oxford, 1987), p. 21.

[47] J. W. Widiatmo, H. Sato, and K. Watanabe, J. Chem. Eng. Data **39**, 304 (1994).

[48] *CRC Handbook of Chemistry and Physics* (CRC, Boca Ratón, Florida, 1986).

[49] C. G. Gray and K. E. Gubbins, *Theory of Molecular Fluids* (Clarendon, Oxford, 1984).

[50] A. L. Benavides, Y. Guevara, and F. del Río, Physica A **202**, 420 (1993).

[51] G. S. Dubey and S. F. O'Shea, Phys. Rev. E **49**, 2175 (1994).

[52] M. Gasset, M. Oñaderra, E. Goormaghteigh, and J. G. Gavilanes, Biochim. Biophys. Acta **1080**, 51 (1991).

[53] H. D. Baehr, F. Klobasa and R. Scharf, Int. J. Thermophys. **10**, 577 (1989).

[54] Y. Kabata, S. Yamaguchi, Y. Takiguchi, and M. Uematsu, J. Chem. Therm. **23**, 671 (1991).

[55] Y. Kabata, S. Yamaguchi, M. Takada and M. Uematsu, J. Chem. Therm. **24**, 1019 (1992).

[56] P. Sauermann, K. Holzapfel, J. Oprzynski, J. Nixdorf, and F. Kohler, Fluid Phase Equil. **84**, 165 (1993).

[57] A. Müller, J. Winkelmann and J. Fischer, J. Chem. Phys. **99**, 3946 (1992).

[58] B. Saager and J. Fischer, Fluid Phase Equil. **72**, 67 (1992).

[59] T. Boublík, Mol. Phys. **73**, 417 (1991).

[60] T. Boublík, Mol. Phys. **76**, 327 (1992).

[61] T. Boublík, Mol. Phys. **77**, 983 (1992).